

Directional anisotropy of secondary-electron bremsstrahlung induced by proton bombardment of thin solid target

著者	石井 慶造
journal or publication title	Physical review. A
volume	15
number	5
page range	2126-2129
year	1977
URL	http://hdl.handle.net/10097/35213

doi: 10.1103/PhysRevA.15.2126

Directional anisotropy of secondary-electron bremsstrahlung induced by proton bombardment of thin solid target

K. Ishii, M. Kamiya, K. Sera, and S. Morita
Department of Physics, Tohoku University, Sendai, Japan

H. Tawara
Department of Nuclear Engineering, Kyushu University, Fukuoka, Japan
 (Received 22 November 1976)

Directional anisotropy around 90° of bremsstrahlung due to secondary electrons ejected by MeV-proton bombardments on a thin Al foil was measured. It is shown that this behavior can be explained by the relativistic retardation effect in bremsstrahlung production.

I. INTRODUCTION

In a previous paper¹ we reported calculations on cross sections and spectra of bremsstrahlung produced by secondary electrons ejected by proton bombardment of thin solid targets and obtained fairly good agreement with the experimental results measured over the bombarding-energy range 1–4 MeV. There we pointed out theoretically the energy-dependent directional anisotropy of the bremsstrahlung and compared with preliminary experimental results at proton energies of 1.5 and 4.0 MeV. In the present work, previous measurements have been extended to other angles and the results compared with calculations including the relativistic retardation effect.

II. EXPERIMENT AND RESULTS

An Al target of 110- $\mu\text{g}/\text{cm}^2$ thickness was set at the center of a scattering chamber of 190-mm diameter. The x rays came out through Mylar-foil windows of the chamber and were detected with a Si(Li) detector, which was set on a goniometer and rotated around the center of the scattering chamber. Corrections for absorption of x rays in the path from the target to the detector and for the detector efficiency have been done as in the previous measurement. A reliable measurement at 30° for 4-MeV proton bombardment was impossible because of a large background due to protons scattered in the forward direction.

Anisotropy of the bremsstrahlung (defined as ratio of the bremsstrahlung-production cross section at an angle θ to that at 90°), together with our previous results, is shown in Figs. 1 and 2 as a function of x-ray energy and in Figs. 3 and 4 as a function of angle. It is clearly seen in these figures that the angular distributions are not symmetric around 90° and the intensity in the forward direction becomes stronger than that in the

backward direction as the bombarding energy increases. As was pointed out in the previous paper,¹ this asymmetry around 90° is considered to be due to the retardation effect in the bremsstrahlung production.

III. THEORETICAL

According to the semiclassical calculation taking into account the relativistic retardation effect,² the production cross section of bremsstrahlung by an electron is given by, instead of Eq. (3) in the previous paper,¹

$$\frac{d\sigma^{\text{br}}}{d(\hbar\omega)d\Omega_L} = \frac{2}{\pi} \frac{Z^2 e^2}{\hbar c} \left(\frac{e^2}{m_e c^2} \right)^2 \left(\frac{c}{v} \right)^2 \frac{1}{\hbar\omega} \times \ln \left(4 \frac{E'_e}{\hbar\omega} \right) \frac{\sin^2 \theta_{\text{br}}}{(1 - \beta \cos \theta_{\text{br}})^4}. \quad (1)$$

The notations in Eq. (1) and the following are the same as in Ref. 1. The last term of this equation, which shows the retardation effect, is reduced to $\sin^2 \theta_{\text{br}} (1 + 4\beta \cos \theta_{\text{br}})$ for $\beta \ll 1$, where $\beta^2 = E'_e / \frac{1}{2} m_e c^2$, E'_e being the kinetic energy of electron which emits the bremsstrahlung. Therefore, the production cross section of bremsstrahlung by secondary electrons produced by proton bombardment, σ^{SEB} , is expressed by, instead of Eq. (5) of Ref. 1,

$$\frac{d\sigma^{\text{SEB}}}{d(\hbar\omega)d\Omega_L} \approx (3C_2 - C_1) \sin^2 \theta_L + 2(C_1 - C_2) + 4 \cos \theta_L \times [2(C_1^R - C_2^R) + (5C_2^R - 3C_1^R) \sin^2 \theta_L], \quad (2)$$

where

$$C_1 = \int dE_e \int dE'_e \int d\theta_e f,$$

$$C_2 = \int dE_e \int dE'_e \int d\theta_e f \cos^2 \theta_e,$$

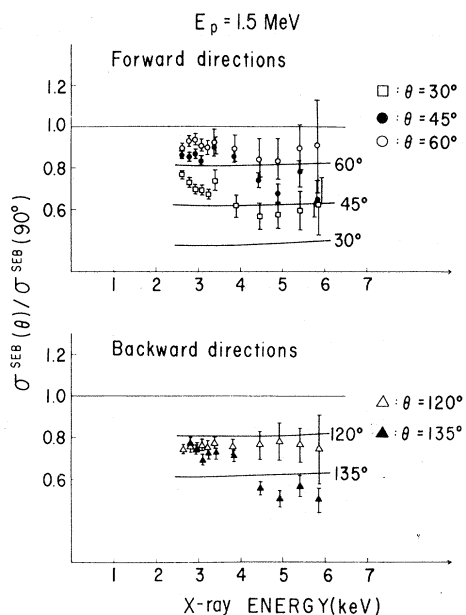


FIG. 1. Anisotropy of secondary-electron bremsstrahlung produced by 1.5-MeV proton bombardment. Ratios of production cross section measured at five angles to that at 90° are plotted as a function of x-ray energy. The solid curves show theoretical predictions without the retardation effect.

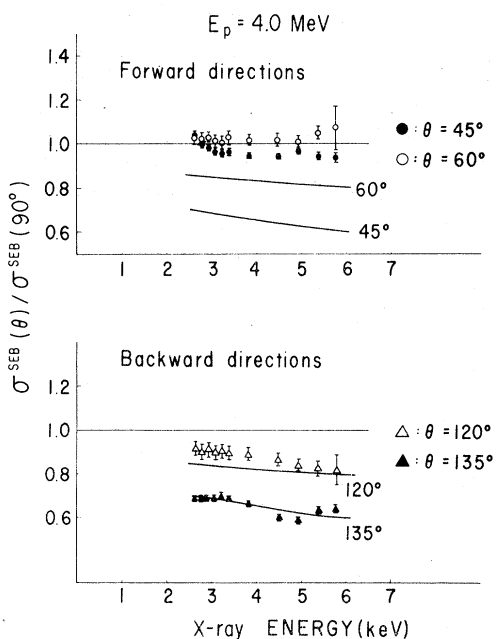


FIG. 2. Same as Fig. 1, except for 4.0-MeV proton bombardment.

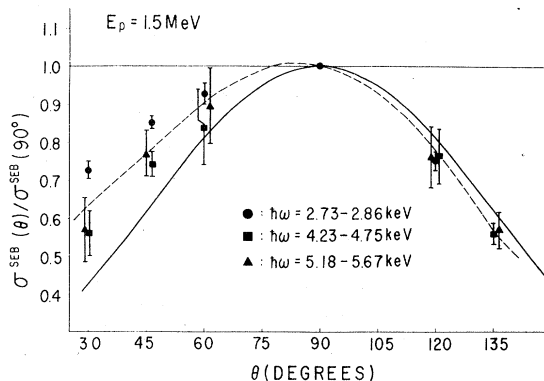


FIG. 3. Anisotropy of secondary-electron bremsstrahlung shown as a function of angle at $E_p = 1.5$ MeV. The solid curve shows theoretical predictions without the retardation effect and the dotted curve represents the theoretical calculation, including the retardation effect, fitted to the experimental results.

$$C_1^R = \int dE_e \int dE'_e \int d\theta_e f \cos\theta_e \beta,$$

and

$$C_2^R = \int dE_e \int dE'_e \int d\theta_e f \cos^3\theta_e \beta,$$

with

$$f(E'_e, E_e, \theta_e) = \frac{3}{8} \frac{d\sigma^{\text{br}}}{d(\hbar\omega)} \left(\frac{-Ndx}{dE'_e} \right) \frac{d\sigma_e}{dE_e d\Omega_e} \sin\theta_e.$$

The last term of Eq. (2) due to the relativistic retardation effect evidently shows that the bremsstrahlung is not symmetric around 90° and the retardation effect vanishes at $\theta_L = 90^\circ$. From Eq. (2), we obtain the anisotropy of bremsstrahlung, $R(\theta_L)$, as

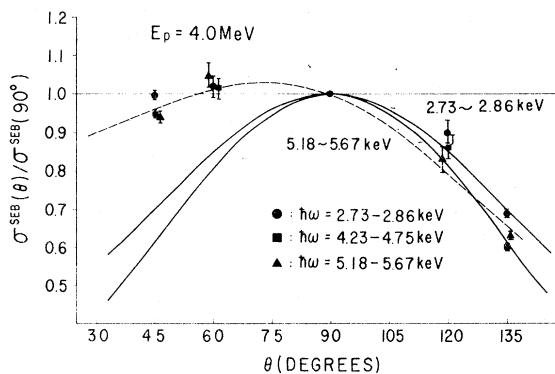


FIG. 4. Same as Fig. 3, except for $E_p = 4.0$ MeV.

$$\begin{aligned}
R(\theta_L) &= \frac{\sigma^{\text{SEB}}(\theta_L)}{\sigma^{\text{SEB}}(90^\circ)} \\
&= (3 - 4P_1) \sin^2 \theta_L + 2(2P_1 - 1) \\
&\quad + 4[2(P_1^R - P_2^R) + (5P_2^R - 3P_1^R) \sin^2 \theta_L] \cos \theta_L,
\end{aligned} \tag{3}$$

where

$$\begin{aligned}
P_1 &= \frac{C_1}{C_1 + C_2}, \quad P_2 = \frac{C_2}{C_1 + C_2}, \\
P_1^R &= \frac{C_1^R}{C_1 + C_2}, \quad P_2^R = \frac{C_2^R}{C_1 + C_2}.
\end{aligned}$$

Also, we obtain

$$R(\theta) + R(180^\circ - \theta) = 2[(3 - 4P_1) \sin^2 \theta_L + 2(2P_1 - 1)], \tag{4}$$

$$\begin{aligned}
R(\theta) - R(180^\circ - \theta) &= 8[2(P_1^R - P_2^R) \\
&\quad + (5P_2^R - 3P_1^R) \sin^2 \theta_L] \cos \theta_L.
\end{aligned} \tag{5}$$

As the angular distribution of ejected electrons has sharp forward maximum in comparison with the distribution $\cos \theta$, we can approximate as follows:

$$C_2 = C_1 \langle \cos^2 \theta_e \rangle \approx C_1 (1 - \langle \theta_e^2 \rangle).$$

Moreover, considering that the energy distribution of ejected electrons decreases very rapidly as the electron energy increases in the higher-energy region which contributes to the production of bremsstrahlung as shown in the previous paper, we can approximate as

$$\begin{aligned}
C_1 &\propto \int_{\hbar\omega}^{\infty} \sigma(E_e) dE_e \int_{\hbar\omega}^{E_e} dE'_e \\
&\approx \int_{\hbar\omega}^{\infty} \sigma(E_e) (E_e - \hbar\omega) dE_e \\
&= \int_0^{\infty} \sigma(E_e) x dx,
\end{aligned}$$

with $E_e = \hbar\omega + x$, and using

$$\left(\frac{E_e}{\hbar\omega}\right)^{1/2} \approx 1 + \frac{1}{2} \frac{x}{\hbar\omega},$$

$$\begin{aligned}
\int_{\hbar\omega}^{\infty} \sigma(E_e) dE_e \int_{\hbar\omega}^{E_e} \beta dE'_e &= \int_{\hbar\omega}^{\infty} \sigma(E_e) \left[E_e \left(\frac{E_e}{\hbar\omega}\right)^{1/2} - \hbar\omega \right] \\
&\quad \times \left[\frac{2}{3} \left(\frac{\hbar\omega}{\frac{1}{2} m_e c^2}\right)^{1/2} \right] dE_e \\
&\approx \left(\frac{\hbar\omega}{\frac{1}{2} m_e c^2}\right)^{1/2} \int_0^{\infty} \sigma(E_e) x dx.
\end{aligned}$$

Thus, we obtain

$$\begin{aligned}
C_1^R &\approx C_1 \left(\frac{\hbar\omega}{\frac{1}{2} m_e c^2}\right)^{1/2} \langle \cos \theta_e \rangle \\
&\approx C_1 \left(\frac{\hbar\omega}{\frac{1}{2} m_e c^2}\right)^{1/2} (1 - \frac{1}{2} \langle \theta_e^2 \rangle)
\end{aligned}$$

and

$$\begin{aligned}
C_2^R &\approx C_1 \left(\frac{\hbar\omega}{\frac{1}{2} m_e c^2}\right)^{1/2} \langle \cos^3 \theta_e \rangle \\
&\approx C_1 \left(\frac{\hbar\omega}{\frac{1}{2} m_e c^2}\right)^{1/2} (1 - \frac{3}{2} \langle \theta_e^2 \rangle),
\end{aligned}$$

and finally, from the definitions following Eq. (3), we obtain

$$P_1^R \approx \frac{1}{2} \left(\frac{\hbar\omega}{\frac{1}{2} m_e c^2}\right)^{1/2} \quad \text{and} \quad P_2^R \approx \frac{1}{2} \left(\frac{\hbar\omega}{\frac{1}{2} m_e c^2}\right)^{1/2} \frac{C_2}{C_1}. \tag{6}$$

IV. COMPARISON WITH EXPERIMENTAL RESULTS AND DISCUSSION

In Figs. 1 and 2, lower-energy parts of the bremsstrahlung, for example $\hbar\omega = 2.73$ – 2.86 keV, show smaller anisotropy, which is considered to be flattened out by multiple scattering of lower-energy electrons inside the target, while the multiple scattering of high-energy electrons is expected to be small. Therefore, the anisotropy measured for higher-energy part ($\hbar\omega = 5.18$ – 5.67 keV) is compared with the calculation.

Experimental values of P_1 can be determined by fitting the measured anisotropy of Eq. (4) and are shown in Table I, together with the calculated one. Experimental values of P_1^R and P_2^R can also be determined by fitting the anisotropy measured at $\theta_L = 45^\circ$ and 135° and at $\theta_L = 60^\circ$ and 120° to Eq. (5)

TABLE I. Values of P_1 for x rays with energy 5.18–5.67 keV.

E_p (MeV)	$\sigma^{\text{SEB}}(45^\circ) + \sigma^{\text{SEB}}(135^\circ)$	$\sigma^{\text{SEB}}(60^\circ) + \sigma^{\text{SEB}}(120^\circ)$	Least-squares	
			method	Calculated
4	0.643 ± 0.19	0.690 ± 0.44	0.652	0.557
1.5	0.585 ± 0.03	0.578 ± 0.082	0.583	0.585

TABLE II. Values of P_1^R and P_2^R for x rays with energy 5.18–5.67 keV.

E_p (MeV)		$\sigma^{\text{SEB}}(45^\circ) - \sigma^{\text{SEB}}(135^\circ)$	Least-squares method	Calculated
		$\sigma^{\text{SEB}}(60^\circ) - \sigma^{\text{SEB}}(120^\circ)$		
4	P_1^R	0.069 ± 0.036	0.068	0.073
	P_2^R	0.041 ± 0.015	0.045	0.065
1.5	P_1^R	0.046 ± 0.033	0.045	0.0728
	P_2^R	0.025 ± 0.014	0.026	0.062

and their approximate theoretical values are estimated from Eq. (6). The results are shown in Table II. Errors shown in these tables were estimated from statistical ones, background subtraction, and corrections for absorption, as we discuss here only the ratios of cross section, and they come mainly from the background subtraction.

In the case of $E_p = 1.5$ MeV, E_p being the incident proton energy, the value of P_1 determined from the least-squares fitting is in good agreement with the calculated one. The values of P_1^R and P_2^R for $E_p = 1.5$ and 4.0 MeV roughly agree with the calculated ones within the errors, except the value of P_2^R for $E_p = 1.5$ MeV, which might be due to the rough approximation of the theoretical estimation. Thus it is found that Eq. (3) including the retardation effect can well reproduce the observed anisotropy.

In the case of $E_p = 4.0$ MeV, it is found from Table I and the relation $P_1 + P_2 = 1$ that $P_2^{\text{exp}} < P_2^{\text{theo}}$ and $C_2^{\text{exp}} < C_2^{\text{theo}}$. It should be noted that the x-ray energy region discussed here corresponds to the region of $E_e < T_m$ for $E_p = 4$ MeV ($T_m = 8.7$ keV) and to that of $E_e > T_m$ for $E_p = 1.5$ MeV ($T_m = 3.3$ keV), T_m being the maximum energy that can be transferred from the incident proton to a free electron and E_e being the energy of ejected electrons from an atom by the incident proton. It has been reported by Rudd *et al.*,³ that experimental angular distributions of ejected electrons at $E_e \approx T_m$ do not show so sharp a forward maximum as predicted by a binary-encounter approximation (BEA) calculation. This fact should be reflected in the calculation of the coefficient C_2 , as $\cos^2\theta_e$ is involved in its defi-

inition following Eq. (2), while C_1 does not depend on the angular distribution of ejected electrons. It is then considered to result in $C_2^{\text{exp}} < C_2^{\text{theo}}$ and $C_1^{\text{exp}} \approx C_1^{\text{theo}}$ at $E_p = 4$ MeV. As $\sigma^{\text{SEB}}(90^\circ) = C_1 + C_2$ from Eq. (2), putting

$$\sigma^{\text{SEB}}(90^\circ) = C_1^{\text{theo}} + C_2^{\text{theo}} P_2^{\text{exp}} / P_2^{\text{theo}}, \quad (7)$$

the calculated cross section in the previous paper becomes smaller by about 10%, showing that the cross sections for $E_p = 4$ MeV shown in Fig. 8 of that paper, which is a little bit larger than the experimental, become in good agreement with the experiment. Good agreement of the anisotropy at $E_p = 1.5$ MeV, where $P_1^{\text{exp}} \approx P_1^{\text{theo}}$, demonstrates the validity of the angular distribution of the BEA theory in the region $E_e > T_m$.

In conclusion, the anisotropy of the bremsstrahlung produced by secondary electrons, especially that for the higher-energy part (where the effect of multiple scattering of electrons is expected to be small), can be explained by the relativistic retardation effect. Moreover, the spectrum for $E_p = 4$ MeV previously reported is consistent with the fact that the angular distribution of ejected electrons has not so sharp a forward maximum as predicted by the BEA calculation.

ACKNOWLEDGMENTS

One of the authors, S. M., would like to express his sincere thanks to National Tsing Hua University in Taiwan for inviting him to take part in discussions with Professor C. C. Hsu and other staff of the University.

¹K. Ishii, S. Morita, and H. Tawara, Phys. Rev. A **13**, 131 (1976).

²J. D. Jackson, *Classical Electrodynamics* (Wiley, New York, 1975), p. 701; A. Sommerfeld, Phys. Z. **10**,

969 (1909).

³M. E. Rudd, C. A. Sautter, and C. L. Bailey, Phys. Rev. **151**, 20 (1966).